Turk J Chem
29 (2005) , 697 – 706.

Characterization of TiO_2 Synthesized in Alcohol by a Sol-Gel Process: The Effects of Annealing Temperature and Acid Catalyst

Funda SAYILKAN[1], Meltem ASİLTÜRK[2], Hikmet SAYILKAN[1]*, Yunus ÖNAL[3], Murat AKARSU[4] and Ertuğrul ARPAÇ[5]

[1] *İnönü University, Faculty of Education, Department of Science, 44280 Malatya-TURKEY*
e-mail: hsayilkan@inonu.edu.tr

[2] *İnönü University, Faculty of Arts and Science, Department of Chemistry, 44280 Malatya-TURKEY*

[3] *İnönü University, Faculty of Engineering, Department of Chemical Engineering, 44280 Malatya-TURKEY*

[4] *Institute für Neue Materialien, D-66123 Saarbrücken-GERMANY*

[5] *Akdeniz University, Faculty of Arts and Science, Department of Chemistry, 07100, Antalya-TURKEY*

Received 26.01.2005

The effects of annealing temperature and hydrolysis catalyst on the crystalline form and crystallite size of TiO_2 prepared by a sol-gel process were investigated. Three types of TiO_2 were synthesized by hydrolysis of titanium(IV)-iso-propoxide with water in n-propanol without catalyst (Type-A) and with HCl as catalyst, where the H^+/Ti^{4+} mol ratio was 0.54 for Type-B and 0.2 for Type-C. Hydrolysis products were thermally treated at 100, 200, 300, 400 and 500 °C for 1 h after drying at room temperature. Characterization of the particles was carried out using XRD, BET, TG/DTA and SEM analysis. The pore size distributions were computed by the DFT plus method. The results showed that the acid catalyst and catalyst/alkoxide ratio have a large effect on the formation of anatase TiO_2. In particular, it was found that anatase phase TiO_2 particles occur at 400 and 500 °C for Type-A TiO_2, while they do so at nearly 200 °C for Type-B and Type-C TiO_2. The crystallite size of Type-A, Type-B and Type-C increased from 17.96 to 19.24 nm, from 12.38 to 15.12 nm and from 10.60 to 12.20 nm, respectively, when the thermal treatment temperature was raised from 400 to 500 °C.

Introduction

Titania (TiO_2) has 3 crystalline forms: anatase, brookite and rutile. Of these forms, anatase TiO_2 has been widely used as a popular catalyst, because of its various merits, such as optical and electronic properties, high photocatalytic activity, low cost, non-toxicity and chemical stability[1−5]. It is well known that TiO_2 is

*Corresponding author

one of the most popular and promising materials in photocatalytic applications due to the strong oxidizing power of its holes, high photostability and redox selectivity[6,7]. The catalytic activity of TiO_2 is dependent on its specific surface area, which is certainly dependent on the crystal size (i.e. the smaller the catalyst, the larger will be its specific surface area). A number of methods for TiO_2 nano-particle preparation have been reported, such as chemical precipitation[8], microemulsion[9], hydrothermal crystallization[10−13] and sol-gel[14−21]. The sol-gel process is the most successful for preparing nanosized metal oxide semiconductors. For example, sol-gel derived TiO_2 powders have been reported to show high catalytic activity due to their fine structure, wide surface area and high porosity.

The sol-gel process is a low temperature route widely used to obtain better ceramics. When the precursor is a transition metal alkoxide, its high reactivity towards water must be controlled to obtain gels. Several methods can be used to do that. For example, the alkoxide can be chemically modified[22]. Another method is to use an acid medium, where the protons limit the condensation and allow gelation[22]. In this process, TiO_2 is usually prepared by hydrolysis, condensation and polycondensation of the titanium alkoxides, $Ti(OR)_4$. In these reactions oxopolymers are formed and then transferred into an oxide network. The overall reaction is usually written as follows:

$$M(OR)_n + n/2H_2O \longrightarrow MO_{n/2} + n/2ROH$$

At present, the reaction scheme proposed by Livage[23] is generally accepted. According to this scheme, the first step comprises quick substitution of one alkoxy group with a hydroxy group by a nucleophilic mechanism:

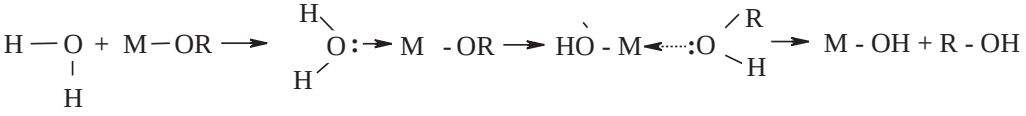

In the second step, oxo- and hydroxo-bridges form during the course of condensation reactions:

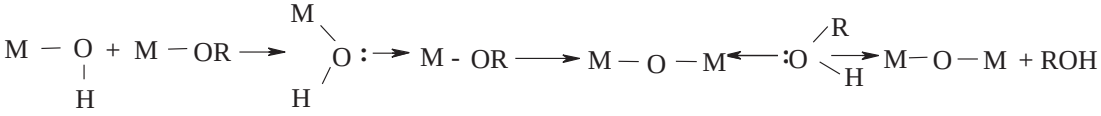

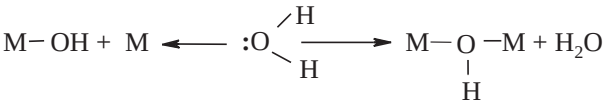

It has been demonstrated that both reactions are quick, and their rates do not differ considerably[24,25]. Condensation results in the formation of oligomeric oxoalkoxides with varying compositions of $Ti_xO_y.OR_{4x-2y}$.

The acid catalyst can influence both the hydrolysis and condensation rates and the structure of the condensed product. Acid serves to protonate negatively charged alkoxide groups, enhancing the reaction kinetics by producing easily removable groups, which can be described as

$$M{-}OR + H_3O^+ \longrightarrow M^+ \longleftarrow :O(HR) + H_2O$$

and eliminating the requirement of proton transfer within the transition state. Generally, inorganic acids such as HCl, HNO_3 and H_2SO_4 are used as acid catalysts. Among these, HCl is the most commonly used. This may be due to the lower electronegativity of the chloride anion compraed to the others[23], and bonding of the chloride ion to the Ti atom as a monodentate ligand, while sulfate and/or nitrate ions can be bonded as bidentate ligands causing a strong interaction between the Ti atom and sulfate and nitrate anions. For this reason, the chloride anion can be removed easily from the metal atom when the hydroxyl ion is attacted to the metal atom. However, inorganic acids have one disadvantage: they cannot be removed from the solution. Therefore, Nass et al.[26] used CO_2 as a catalyst, since it gives an acidic reaction with water and can easily be removed from solution. On the other hand, organic acids cannot be favored as catalysts, since they react easily with metal alkoxides and these are generally bonded to the metal atom as bidentate ligands. In these reactions alkoxide groups are replaced by carboxylate groups.

In the present study, the preparation of nanocrystallite-TiO_2 particles by a sol-gel process was aimed. For this purpose, the effects of annealing temperature and hydrolysis catalyst on the crystalline form and crystallite size of TiO_2 were investigated.

Experimental

Chemicals

The following commercial reagents were used without further purification. Titanium(IV)-iso-propoxide, $[Ti(OPr^i)_4]$, (97%, Alpha) was used as starting precursor for synthesizing crystalline TiO_2 particles. Hydrochloric acid (HCl) (37%, Merck) was used as a catalyst for alkoxide hydrolysis. n-Propanol (99%, Riedel de Haen) stored over molecular sieves (Fluka, 3Å XL8) was used as a solvent. Deionized water was used for the hydrolysis of $Ti(OPr^i)_4$.

Apparatus

X-ray diffraction (XRD) patterns of all types of TiO_2 particles were obtained by Rigaku Geigerflex D-Max/B model diffractometer using CuK_α radiation, with a scanning speed of 0.02°/min at 2θ-steps. The specific surface area and average pore diameter of particles were measured via nitrogen adsorption, using a Micromeritics ASAP 2000 model BET analyzer. A digital instrument LEO EVO 40 model scanning electron microscope (SEM) was used to examine the morphology of the particles. Thermogravimetric analysis (TGA) and differential thermal analysis (DTA) of the hydrolyzed and gently dried products were performed by a Schimadzu System-50 model thermal analyzer. Heat treatment of samples was performed at 10 °C/min in a flowing air environment.

Procedure

Anatase TiO_2 particles were synthesized by the hydrolysis reaction of $Ti(OPr^i)_4$ with water, either adding different amounts of acid catalyst or not.

Synthesis of anatase TiO_2 particles without acid catalyst

Titanium(IV)-iso-propoxide (TIP) (100 g) was added to n-propanol (200 g) and the mixture was stirred for 5 min using a magnetical stirrer operating at 500 rpm. After stirring, a mixture of water (25.33 g) and n-propanol (127 g) was added to the alkoxide solution by burette. The rate of addition was kept at 1 mL/min. The molar ratio of H_2O/TIP was 4. After adding the water/alcohol solution, the mixture was stirred for about 24 h at room temperature. The solid product was separated by centrifuging, and dried at room temperature for a night. The dried product then underwent heat treatment at 100-500 °C for 1 h. Thus, Type-A TiO_2 particles were obtained.

Synthesis of anatase TiO_2 particles with acid catalyst

Titanium(IV)-iso-propoxide (TIP) (100 g) was added to n-propanol (200 g) and the mixture was stirred for 5 min using a magnetical stirrer operating at 500 rpm. After stirring, a mixture of HCl (6.94 g) and n-propanol (20 g) was added to the TIP/n-propanol mixture by burette at the same rate as described above. The molar ratio of HCl/TIP was 0.54. The mixture was stirred for 30 min. After stirring, a mixture of water (25.33 g) and n-propanol (127 g) was added to the alkoxide solution by burette. The rate was kept at 1 mL/min. The molar ratio of H_2O/TIP was 4. After adding the water/alcohol solution, the mixture was stirred for about 24 h at room temperature and a gel product was obtained. The gel product was separated by centrifuging, and dried at room temperature for a night. The dried product was then heat treated at 100-500 °C for 1 h. Thus, Type-B TiO_2 particles were obtained.

The other type of TiO_2 (Type-C) was synthesized as described above except that the molar ratio of HCl/TIP was 0.2.

Results and Discussion

XRD patterns of the heat-treated TiO_2 at different temperatures are shown in Figure 1a for Type-A TiO_2, Figure 1b for Type-B TiO_2 and Figure 1c for Type-C. Type-A TiO_2 was primarily in the amorphous phase until 400 °C. It was observed that annealing at 400 and 500 °C leads to the formation of the anatase phase. Type-B TiO_2 powders were mainly in the amorphous phase until 200 °C. However, when raising the heating temperature from 200 to 500 °C, Type-B TiO_2 particles were transformed into the anatase phase. Type-C TiO_2 was only in the amorphous phase at 100 °C and was then transformed into the anatase phase at 200 °C (Figure 1c). When Figure 1a is compared with Figures 1 b and c it is observed that the reflections that occurred in the non-acidic medium are greater than those in the acidic medium. These reflections show that crystallization is not completed in this medium. When the annealing temperature of 200 °C is considered, the reflections that occurred in Type-B are greater than those in Type-C, showing once more that crystallization of Type-B is not fully completed. However, the other crystalline phases of TiO_2, brookite and rutile phases, were not detected at all temperatures, meaning that an absolute anatase TiO_2 crystalline phase was obtained. These results suggested that acid catalyst and its amount play significant roles in the synthesis of the anatase crystalline form of TiO_2 at low temperatures. It has been reported that high acid concentrations (e.g., when the H^+/alkoxide mol ratio approximates to unity) severely retard the condensation kinetics[23] and cause the formation of a gel product. After treatment at 200 °C, Type-A and Type-B did not constitute sol with water, while Type-C did. Briefly, it was found that the acid and its

amount have significant effects on the preparation of TiO_2 sol.

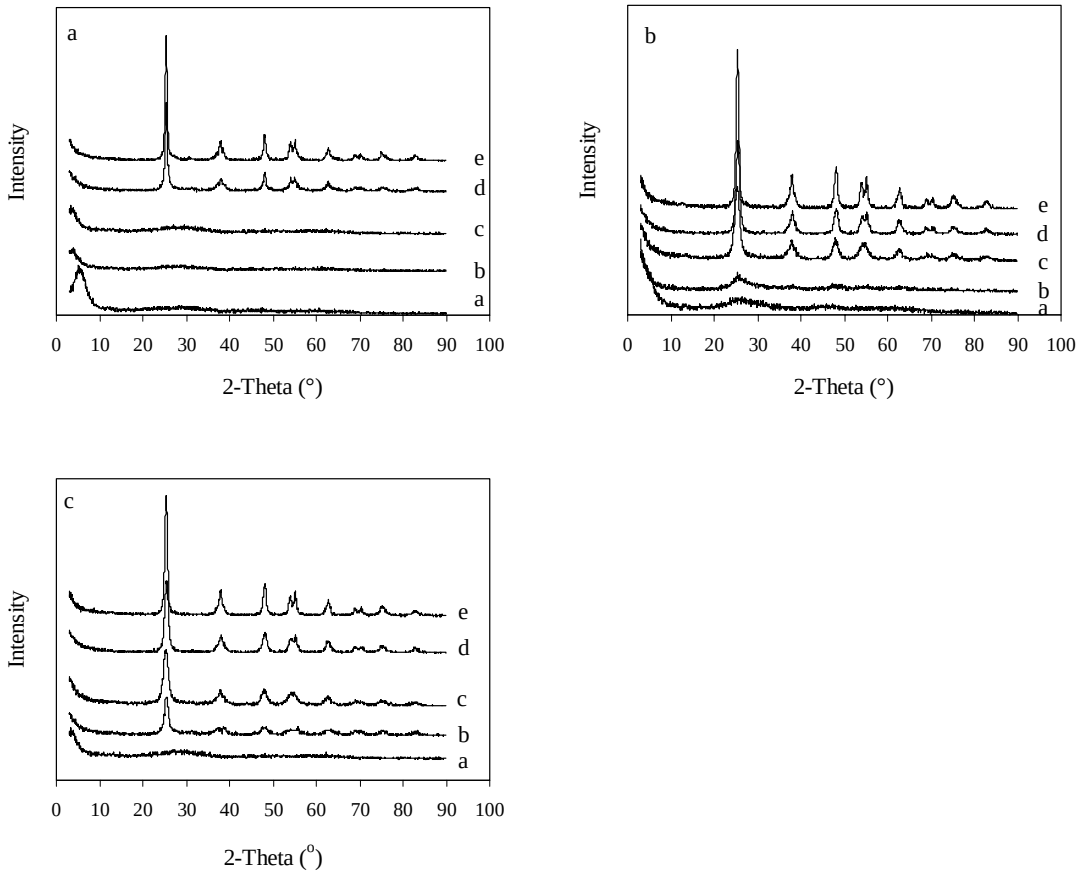

Figure 1. XRD patterns of Type-A TiO_2 (a), Type-B TiO_2 (b) and Type-C TiO_2 (c) nanoparticles treated at 100 (a), 200 (b), 300 (c), 400 (d) and 500 °C (e).

The BET surface areas and average pore diameter for Type-A, Type-B and Type-C TiO_2 are shown in the Table as a function of the annealing temperature from 300 to 500 °C. The Table also lists the average crystallite sizes of Type-A, Type-B and Type-C TiO_2, as calculated from the XRD peak, according to Scherrer's equation:

$$D = 0.9\lambda \ / \ (\beta \cos\theta)$$

where D is the average crystallite size (nm), λ is the X-ray wavelength used ($\lambda = 1.54056$ Å), θ is the angle of diffraction, and β is a full width at half the maximum of the diffraction line observed ($2\theta = 25.3$) in radians.

The Table, shows Type-C and Type B-TiO_2 are in the anatase phase at 200 and 300 °C, respectively, whereas Type-A TiO_2 particles are still amorphous, even at 400 °C. The phase transition of Type-A particles from amorphous to anatase occurs at 500 °C. These results indicate that the hydrolysis catalyst and its amount play important roles in the formation of anatase-TiO_2 particles at low temperatures. The crystallite size of Type-A TiO_2 was larger than that of Type-B and Type-C as a function of temperature, mainly depending on the aggregation that occurred in non-hydrolysis catalyst medium. As the crystallite

size increased, the specific surface area decreased, while the average pore diameter increased. Poresize distributions, as calculated by the DFT-plus method, for Type-A, Type-B and Type-C TiO_2 treated at 500 °C, are plotted in Figure 2. When surface area and pore volume are considered, pores of all the types of particles have the same properties. As seen from Figures 2c and d, the maximum pore size distribution of Type-B TiO_2 is between 3 and 15 nm and the micropore structures are observed at 1-2 nm. Type-A TiO_2 has more micropores than Type-B and Type-C TiO_2 (Figures 2a, b). It was also found that the maximum pore size distribution of Type-A TiO_2 with 3-8 nm is more homogeneous than that of Type-B and Type C TiO_2. Type-A TiO_2 has also some meso- and macropores with 30-100 nm. Type-B and Type-C TiO_2 do not have these types of pores. The maximum pore size distribution of Type-C TiO_2 is between 3 and 16 nm and the micropore structures were observed at 1.2-2.5 nm. Two small sharp peaks showed that Type-C TiO_2 has more micropores than Type-B. These results are consistent with the average pore diameter calculated from the BET and BJH analysis as 9.06 nm and 7.54 nm for Type-A TiO_2, and 4.94 nm and 6.14 nm for Type-B TiO_2, respectively, suggesting that HCl catalyst is responsible for the formation of homogeneous pores.

Table. The textural properties and phase composition of TiO_2 particles treated at different temperatures.

Particle type	Temperature (°C)	Crystalline phase	Crystallite size (nm)	SSA* (m^2/g)	APD** (nm)
Type-A	300	Amorphous	-	-	-
Type-B	300	Anatase	10.36	242.67	3.35
Type-C	300	Anatase	9.80	130.10	2.68
Type-A	400	Anatase	17.96	8.14	2.38
Type-B	400	Anatase	12.38	84.91	6.21
Type-C	400	Anatase	10.60	53.19	5.10
Type-A	500	Anatase	19.24	4.25	4.94
Type-B	500	Anatase	15.12	59.44	9.06
Type-C	500	Anatase	12.20	45.38	7.40

*SSA: Specific surface area

**APD: Average pore diameter

The TG results, given in Figure 3a for Type-A TiO_2, showed that the alkoxide groups bonded to the Ti-atom can be removed by heating to 460 °C in air. Total weight loss of these particles finished at 460 °C, while it finished at 290 °C for Type-B TiO_2 (Figure 3c). Weight loss for Type-A TiO_2 was observed at 3 different temperatures, namely, below 150 °C, at 150 - 260 °C and at 260 - 460 °C. In the first region (below 150 °C) the weight loss (9.7%) is thought to result from the evaporation of physically adsorbed water and/or the organic solvent as n-propanol. The weight loss (9.37%) at 150 - 260 °C is attributed to carbonization or combustion of the alkoxide groups bonded to the Ti-atom. The weight loss (9.57%) at 260 - 460 °C is due to the removal of different forms of chemisorbed hydroxyl groups and further combustion of the remaining organic groups. No significant thermal event occurs after 460 °C. In the DTA results of Type-A TiO_2 (Figure 3b), the broad endothermic and exothermic peaks observed at about 105 and 280 °C, matching the weight losses, are attributed to the removal and combustion of physically adsorbed water, chemisorbed hydroxyl and alkoxide groups. According to the TGA results for Type-B TiO_2, the total weight loss finished at nearly 290 °C. At the former temperature, the weight loss (6.7%, broad endothermic peak at 100 °C, Figure 3d) is thought to result from the evaporation of physically adsorbed water and/or the organic solvent as n-propanol. At the latter temperature, the weight loss (18.7%, sharp and strong exothermic peak

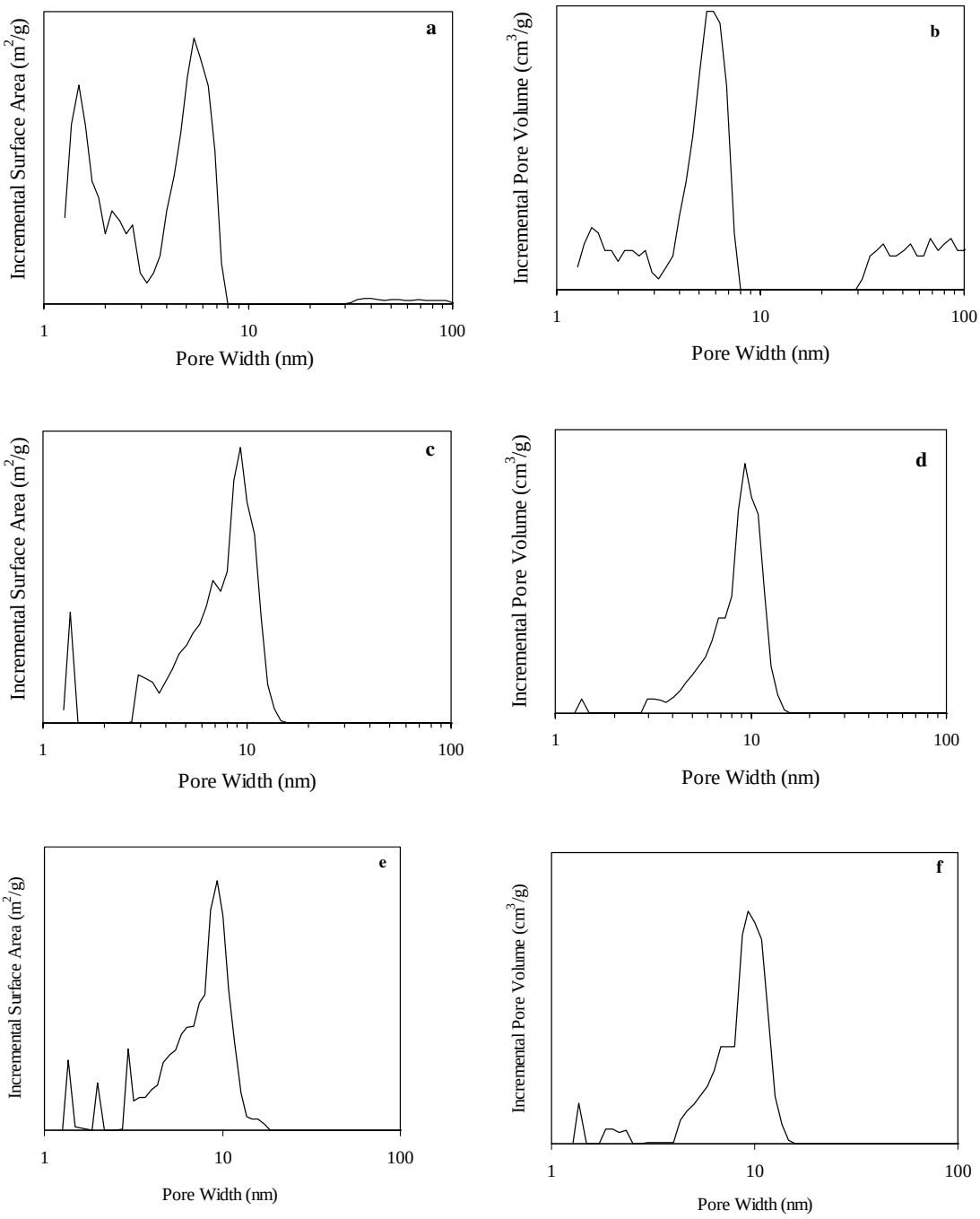

Figure 2. Pore-size distributions of Type-A (a,b), Type-B (c,d) and Type-C (e,f) TiO_2 nanoparticles treated at 500 °C.

at 285 °C) is attributed to the carbonization or combustion of the alkoxide groups bonded to the Ti-atom. The very small peak observed at 510 °C in the TGA curve and the sharp exothermic peak at 500 °C in the DTA curve correspond to 0.4% weight loss, attributed to phase transformation from brookite to anatase.

Typical SEM micrographs of the samples obtained from Type-A and Type-B TiO_2 heated at 500 °C for 1 h show morphologies clearly different from each other (Figure 4). Figure 4b shows that Type-B TiO_2 has a more uniform and smooth surface, and no agglomeration is observed, compared to Type-A TiO_2 (Figure 4a). Type-A TiO_2 has a less uniform surface like a sponge. In this sample, smaller particles likely aggregate to form larger particles with non-spherical shapes. The agglomerations are irregular and the aggregates are nearly 0.5 and 3 μm in size. However, according to the XRD results, these particles have only an anatase crystalline phase at high temperatures and their crystallite sizes are nearly 17 and 20 nm. These results reveal the role of the hydrolysis catalyst, providing more homogeneity and preventing agglomeration.

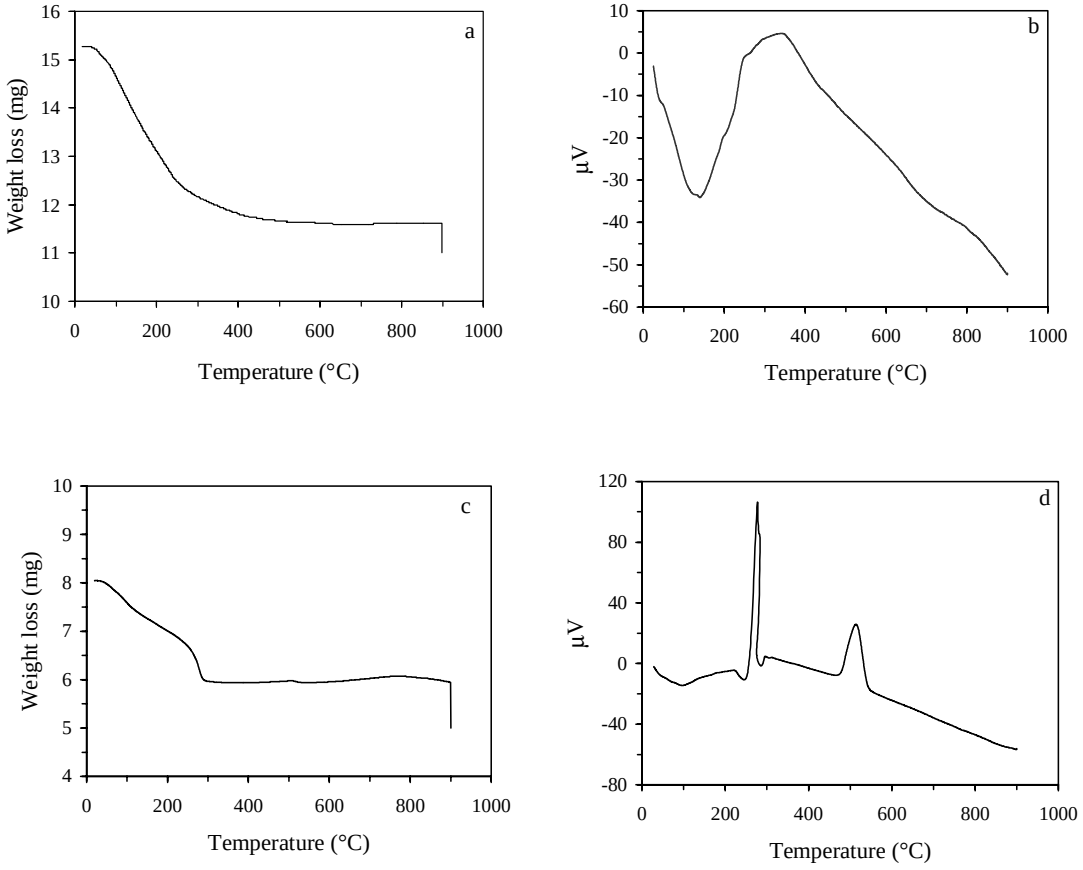

Figure 3. TG/DTA curves of Type-A (a,b) and Type-B (c,d) TiO_2 nanoparticles.

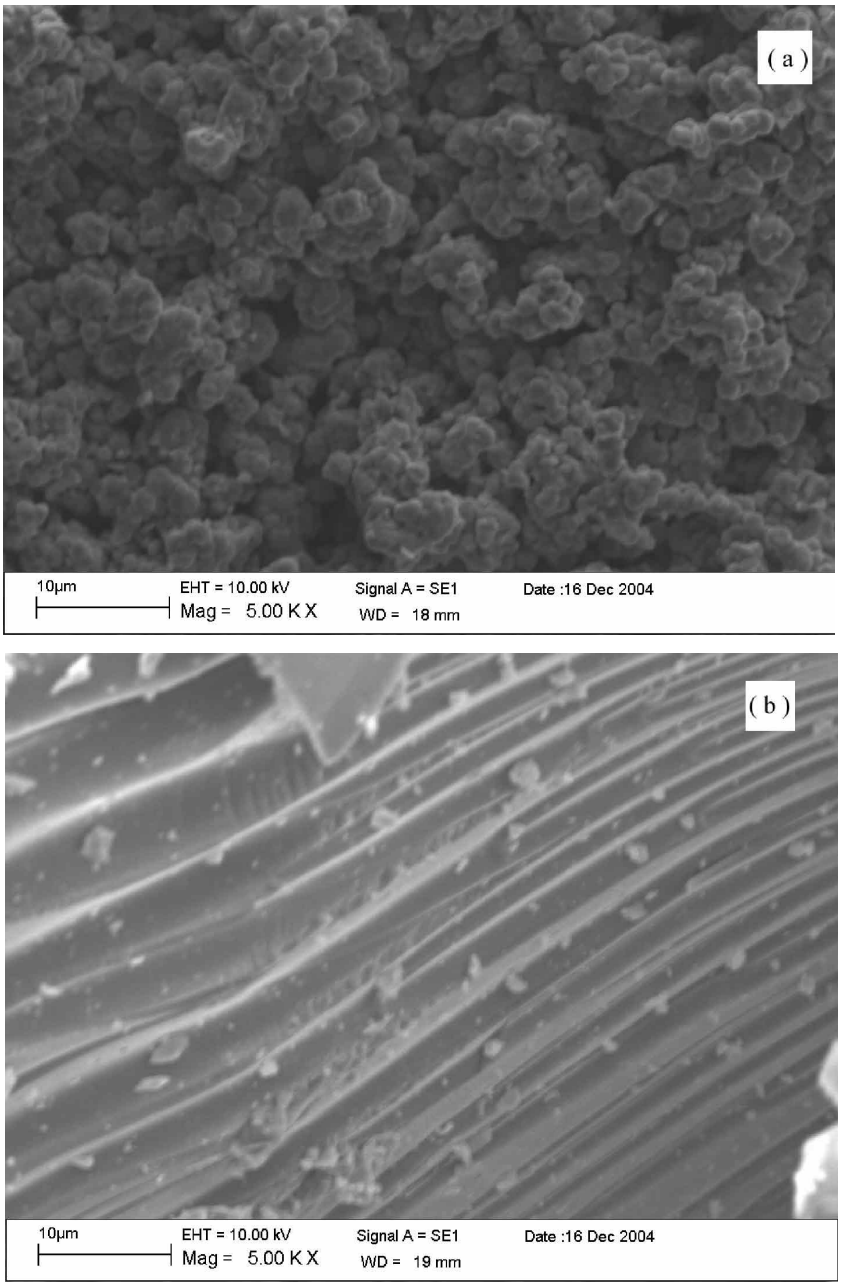

Figure 4. Typical SEM micrographs of Type-A (a) and Type-B (b) TiO_2 nanoparticles treated at 500 °C.

Conclusions

Nanocrystallite-TiO_2 particles in the anatase phase were synthesized in the presence and in the absence of acid catalyst by a sol-gel process. It was found that HCl, as a hydrolysis catalyst, plays an important role in the formation of the anatase crystalline form of TiO_2 at low temperatures. Smaller crystallite size was obtained with the aid of the catalyst at low annealing temperatures. TiO_2 synthesized in acidic media has only micropores, whereas TiO_2 synthesized in the absence of the cataylst has micro-, meso- and macropores.

Acknowledgment

This study was supported by a research grant from İnönü University, Management Unit for Scientific Research Projects (BAPB-2004/01), Malatya, Turkey.

References

1. A. Rammal, F. Brisach and M. Henry, **C. R. Chimie 5**, 59-66 (2002).
2. P.V. Kamat, **Chem. Rev. 93**, 267-300 (1999).
3. A. Mills, G. Hill, S. Bhopal, I.P.Parkin and S.A. O'Neill, **J. Photochem. Photobiol. A: Chemistry 160**, 185-194 (2003).
4. P.S. Awati, S.V. Awate, P.P. Shah and V. Ramaswamy, **Catal. Comm. 4**, 393-400 (2003).
5. R. Zhang, L. Gao and Q. Zhang, **Chemosphere 54**, 405-411 (2004).
6. W.W. So, S.B. Park and S.J. Moon, **J. Mater. Sci. Lett. 17**, 1219-1222 (1998).
7. J. Yang, S. Mei and J.M.F. Ferreira, **Mater. Sci. Eng. C 15**, 183-185 (2001).
8. S. Jeon and P.V. Braun, **Chem. Mater. 15**, 1256-1263 (2003).
9. Y. Bessekhouad, D. Robert and J.W. Veber, **J. Photochem. Photobiol. A: Chemistry 157**, 47-53 (2003).
10. M.M. Yusuf, H. Imai and H. Hirashima, **J. Sol-Gel Sci. Technol. 25**, 65-74 (2002).
11. Y.V. Kolen'ko, B.R. Churagulov, M. Kunst, L. Mazerolles and C. Colbeau-Justin, **App. Catal. B: Environ. 54**, 51-58 (2004).
12. B. O'Regan and M. Gratzel, **Nature 353**, 737 (1991).
13. H. Kominami, J. Kato, M. Kno, Y. Kera and B. Otani, **Chem. Lett.** 1051 (1996).
14. Y. Diaoued, S. Badilescu, P.V. Ashirt, D. Bersani, P.P. Lottici and J. Robichaud, **J. Sol-Gel Sci. Technol. 24**, 255-264 (2002).
15. C. Su, B.Y. Hong and C.M. Tseng, **Catal. Today 96**, 119 (2004).
16. C.C. Wang and J.Y. Ying, **Chem. Mater. 11**, 3113 (1999).
17. K.Y. Jung and S.B. Park, **Mater. Lett. 58**, 2897 (2004).
18. H. Bala, J. Zhao, Y. Jiang, X. Ding, Y. Tian, K. Yu and Z. Wang, **Mater. Lett. 59**, 1937 (2005).
19. H. Zhang and J.F. Banfield, **Chem. Mater. 14**, 4145 (2002).
20. W. Hao, S. Zeng, C. Wang and T. Wang, **J. Mater. Sci. Lett. 21**, 1627 (2002).
21. M.M. Yusuf, H. Imai and H. Hirashima, **J. Sol-Gel Sci. Technol. 25**, 65 (2002).
22. C.J. Brinker and G.W. Scherer, **Sol-Gel Science. The Physics and Chemistry of Sol-Gel Processing** Academic Press, Boston, p. 52 (1990).
23. J. Livage, M. Henry and C. Sanchez, **Progr. Solid State Chem. 18**, 259 (1988).
24. M.T. Harris, A. Singhal, J.L. Look, J.R. Smith-Kristensen, J.S. Lin and L.M. Toth, **J. Sol-Gel Sci. Techn. 8,** 41 (1997).
25. J. Blanchard, S. Barboux-Doeuff, J. Maquet and C. Sanchez, **New J. Chem. 19**, 929 (1995).
26. R. Nass, E. Arpaç, W. Glaubitt and H. Schmidt, **J. Non-Cryst. Solids 121**, 370 (1990).